ADVANCES IN ATMOSPHERIC SCIENCES, VOL. 27, NO. 5, 2010, 1014–1024

Near-equatorial Typhoon Development: Climatology and Numerical Simulations

YI Bingqi (伊炳祺) and ZHANG Qinghong* (张庆红)

Department of Atmospheric Sciences, School of Physics, Peking University, Beijing 100871

(Received 27 April 2009; revised 23 November 2009)

ABSTRACT

The climatology of near-equatorial typhoons over the western-north Pacific are fully investigated using the JTWC (Joint Typhoon Warning Center) typhoon record from 1951 to 2006. The result shows that there are seasonal and decadal variations, as well as a distinctive spatial distribution, of such events. Among them, Typhoon Vamei is an example of a near-equatorial typhoon that occurred near Singapore in December of 2001. Using the WRF (Weather and Research Forecast) model, we attempt to find out how the well known "wind surge" of this event contributes to the development of Typhoon Vamei. It is found that the strong wind surge not only helps to provide advection of positive vorticity to Vamei between 800 and 500 hPa, but also increases the convective instability of the lower troposphere, and thus helps to induce convective outbreaks and rapid intensification. Furthermore, sensitivity experiments show that terrain and the land-sea distribution have very limited effects on the formation of Typhoon Vamei in the simulation, but an adequate Coriolis parameter (f) is still needed for the development of Vamei.

Key words: near-equatorial typhoon, wind surge, Coriolis parameter

Citation: Yi, B. Q., and Q. H. Zhang, 2010: Near-equatorial typhoon development: Climatology and numerical simulations. *Adv. Atmos. Sci.*, **27**(5), 1014–1024, doi: 10.1007/s00376-009-9033-3.

1. Introduction

Near-equatorial tropical cyclones make up only a very small portion of all tropical cyclones, and even fewer of these can further intensify into typhoons at low latitudes. But these storms are still important and are also very challenging to simulate, because they define the extreme conditions for tropical cyclone genesis dynamics. Formerly, there has been some investigation into near-equatorial typhoons. Fortner (1958) was the first to summarize the characteristics of near-equatorial typhoon Sarah (1956) using the data from aerial weather reconnaissance. Based on some statistical study, Holliday and Thompson (1986) concluded that the secondary directional wind shear zone between the equator and 5 degrees north might have something to do with the near-equatorial typhoon genesis. Particularly concerning Typhoon Vamei (2001), some research has been done to investigate the genesis of this rare event. Chang et al. (2003) has pointed out that the strong and persistent cold surge in December 2001 provided a source for background cyclonic vorticity and was crucial for the genesis of Typhoon Vamei (2001). Their conclusion showed that the interaction of the weak Borneo Vortex and the persistent northeast cold surge resulted in this near-equatorial typhoon formation. They further noted that the terrain and land-sea distribution around the South China Sea area might be also an important factor. Juneng et al. (2007) speculated that the higher sea surface temperature was a potential reason for the intensification of typhoon Vamei based on TRMM satellite observations. Chambers and Li (2007) investigated the physical mechanism for the genesis of Vamei based on an MM5 model simulation. The analysis of PV (potential vorticity) and the vorticity equation showed that the rapid intensification process had much to do with the merging of the typhoon system and the mesoscale vortex. They concluded that the formation of Typhoon Vamei was due to the interactions between the large-scale environmental background field and the mesoscale systems.

Although there have been three papers discussing Typhoon Vamei (2001) based on observational and modeling analysis, many questions still remain un-

*Corresponding author: ZHANG Qinghong, qzhang@pku.edu.cn

© China National Committee for International Association of Meteorology and Atmospheric Sciences (IAMAS), Institute of Atmospheric Physics (IAP) and Science Press and Springer-Verlag Berlin Heidelberg 2010

solved. How could Vamei form within five degrees from the equator, whereas this is commonly acknowledged as the "forbidden zone" for typhoons? Why did mesoscale systems merge with the pre-Vaimei system? Is there any other factor involved apart from the dynamical effect of the wind surge as illustrated by earlier research (Gray, 1968; 1998)? We try to use both statistical analysis and numerical model simulation to answer these questions. This paper is organized as follows: in section 2, we will investigate the climatology of the genesis of historical near-equatorial typhoons. A brief introduction of the model and data is given in section 3. Section 4 describes the validation of the results of model simulation. And section 5 discusses the effects of wind surge, terrain, land-sea distribution and Coriolis force on Vamei genesis based on the model result. Finally, a summary is given in section 6.

2. Statistical analysis of near-equatorial typhoons over the Western North Pacific during 1951–2006

Here, we refer to near-equatorial typhoons (tropical storms) as those storms that reach typhoon (tropical storm) intensity within 6 degrees of the equator. By use of typhoon best-track data from the Joint Typhoon Warning Center (JTWC, Joint Typhoon Warning Center, 2009), the annual frequency and seasonal variation of near-equatorial typhoons and tropical storms over the Western North Pacific (WNP) from 1951 to 2006 were analyzed. These results are shown in Figs. 1 and 2, respectively.

It is quite evident from Fig. 1 that the most frequent occurrence of near-equatorial typhoons is in northern hemisphere winter/early spring in the WNP. March is the month with the highest frequency of near-equatorial tropical storms, while the winter months (December and January) have the maximum number of near-equatorial typhoons. On the contrary, near-equatorial typhoons never occur in the summer months (June, July, and August). Accordingly, the frequency of near-equatorial tropical storms decreases sharply from 7 in March to 0 in August. This temporal distribution is quite different from that of typhoons which form relatively further away from the equator.

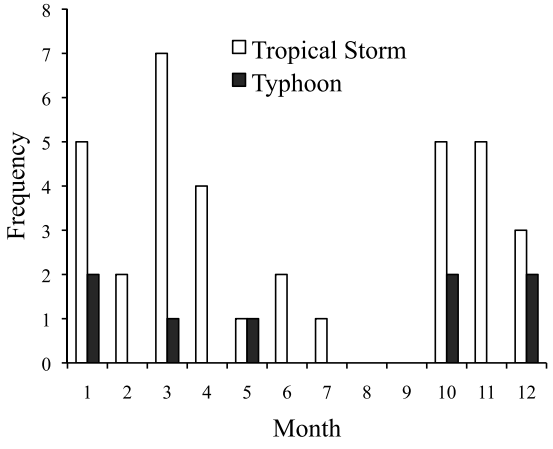

Fig. 1. Seasonal variation of near-equatorial typhoon (tropical storm) frequency over WNP.

Figure 2 shows that there are decadal changes in near-equatorial tropical cyclones from 1951 to 2006. After a period of multiple occurrences of near-equatorial typhoons in the 1950s, a near-equatorial typhoon happened only approximately once every 11 years. Among these events, the frequency of near-equatorial tropical storms is highest in 2001, and the nearest typhoon to the equator in history also appeared in this year, at the latitude of 1.5°N (Table 1).

Table 1 shows the spatial distribution of near-equatorial typhoons over the WNP by name, date, latitude and longitude, as well as their relationship to ENSO events over the WNP. These near-equatorial typhoons mainly generate in a domain that is 40° wide and far away from terrain and continents, with the exception of Typhoon Vamei (2001). It is very clear from the table that near-equatorial typhoon genesis has little to do with ENSO events. There is near-equatorial typhoon genesis regardless of whether ENSO is in the warm, cold, or neutral phase. This is quite different from the conclusion of other research that has found La Nina years tend to bring more typhoon genesis over the South China Sea (Wang et al., 2007).

Gray (1968) pointed out that tropical cyclone development requires a non-negligible Coriolis force, positive low-level rotation, minimal vertical wind shear of the tropospheric horizontal wind, warm ocean surface temperatures (>26.5°C), a potentially unstable atmosphere below 500 hPa, and large relative humidity at mid-levels. NCEP/NCAR reanalysis data (Kalnay et al., 1996, Kanamitsu et al., 2002) are used here to investigate the climatology and anomalies of environmental condition before the genesis of near-equatorial typhoons. Sea surface temperature data come from Extended Reconstructed Sea Surface Temperature (ERSST) data (Smith et al., 2008). Vertical wind shear of the tropospheric horizontal wind is calculated between 850 hPa and 200 hPa. Potential instability is calculated as the equivalent potential temperature difference between the surface and 500 hPa. We compare fields related to these environmental conditions around the typhoon in two days before each of the eight near-equatorial typhoons with that of the monthly 30-year climatological mean. The results of analysis of Gray's six conditions except for

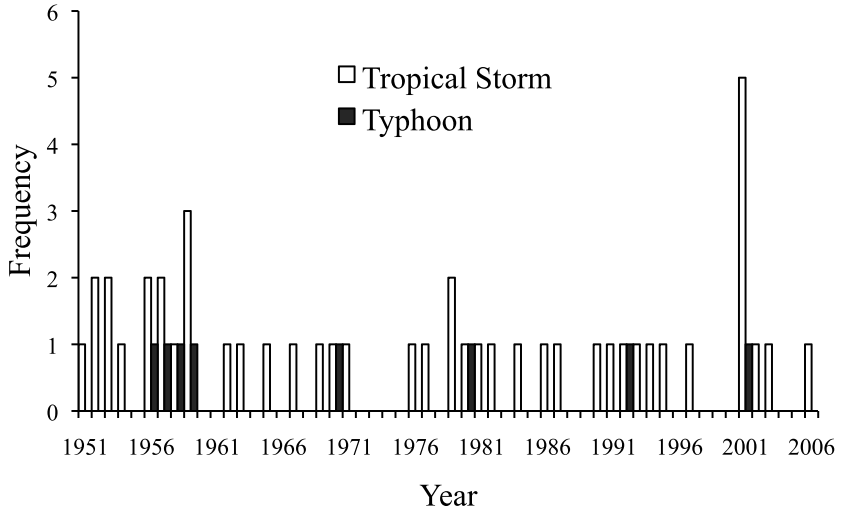

Fig. 2. Annual number of Tropical Cyclones developing within 6° of the equator over the Western North Pacific from 1951 to 2006.

Table 1. Near-equatorial typhoons over the WNP (1951–2006).

Typhoon name	Date	Latitude (°N)	Longitude (°E)	ENSO event
Sarah	0600 UTC 24 March 1956	3.3	146.8	Cold
Trix	0000 UTC 3 May 1957	5.5	155.6	Warm
Ophelia	0600 UTC 7 January 1958	6.0	170.0	Warm
Harriet	0600 UTC 25 February 1959	5.4	150.9	Neutral
Kate	1200 UTC 15 October 1970	4.3	137.4	Cold
Wynne	0000 UTC 4 October 1980	6.0	152.2	Neutral
Axel	1800 UTC 7 January 1992	5.8	169.0	Warm
Vamei	0000 UTC 27 December 2001	1.5	105.1	Neutral

Table 2. Summary of changes of five environmental conditions related to typhoon genesis, from the time before the genesis of near-equatorial typhoons.

	Climatology	Anomalous condition before near-equator typhoon genesis
Relative vorticity at lower level	Positive relative vorticity are found over broad area within 5° of WNP	Positive anomaly are found before storm genesis
Vertical wind shear	Low vertical wind shear are found within 0°–10°N and 130°–170°E	No anomaly is found
Sea surface temperature	The sea surface temperature is higher than 28°C over most area within 10°C in WNP	No anomaly is found except that near-equatorial typhoon genesis in winter always formed in an area with relatively lower SST or with strong SST gradient
Potential instability	High potential instability is always found near equator in WNP	Positive anomaly is found in association with wind surge
Relative humidity at mid-level	The relative humidity is found to be greater than 40% near the equator in WNP	Relative humidity is found to be greater than 60%

the Coriolis force are provided in Table 2. Other than the sea surface temperature and vertical wind shear conditions, the other conditions satisfy Gray's criteria over a broad area of the WNP a region of 5° away. There were more significant anomalous conditions for the low-level vorticity, conditional potential instability, and mid-level relative humidity. The relative humidity before near-equatorial typhoon genesis is greater than 60%, which is higher than the climatic mean of 40%. Cold wind surges are also found before near-equatorial typhoons genesis. The wind surges are found to be associated with positive relative vorticity advection, as well as with vertical instability increase near where the near-equatorial typhoons formed. The role of cold wind surges in tropical cyclone development will be discussed later in this paper.

3. Model and data description

The model used for simulation here is the Weather Research Forecast model (WRF) Version 2.2 (Skamarock et al., 2007), which contains three domains. The horizontal resolutions of the three domains (Fig. 3) are 27 km, 9 km, and 3 km respectively. There are 31 levels in the vertical direction. The outer two domains begin simulation from 0000 UTC 25 December 2001 and run for 60 hours. The inner-most domain begins time steps starting 12 hours later than the outer domains. The main physical schemes used in this simulation include: Lin microphysical process scheme (Lin et al., 1983), Noah land surface model scheme (Chen and Dudhia, 2001), Monin-Obukhov (Janjic Eta) scheme (Janjic, 2002) and Kain-Fritsch (New Eta) cumulous scheme (Kain and Fritsch, 1993). No bogus vortex is added in the simulation. The simulation was initialized using the NCEP global tropospheric analyses, which is available at 6-hourly intervals and has a resolution of 1°×1°.

Apart from the conventional settings in the model, we used a Four Dimensional Data Assimilation (FDDA) Grid Nudging technique (Stauffer and Seaman, 1994) in the simulation. Earlier research (Stauffer and Seaman, 1994) has proven that FDDA Nudging is a method that can combine a complete physical model with observations to reduce the modeling error, improve the model boundary conditions, and relieve the spin-up problem during initialization. In order to fully make use of these advantages while also preventing against possible drawbacks of the FDDA technique, we use one-way nesting between the three domains and only use FDDA in the outer-most domain (27 km) for the first 12 hours; diagnosis and analysis are based on the results of the other two domains (9 km and 3 km). The results show that the FDDA Nudging technique significantly reduces model deflection and improves the track and intensity of the modeled typhoon (not shown).

4. Model verifications

Figure 3 gives the comparison between the simulated typhoon track and the JTWC best track. Clearly, the simulated typhoon track is in good agreement with the JTWC best track. Both show westward parallel movement. Generally, the simulated typhoon track only deflected to the north by about 0.5°. However, the simulated typhoon tends to move slower, and thus the time of landfall is lagged by 3–6 hours as compared with the best track.

The simulated intensity of the typhoon also shows good agreement with the best track (Fig. 4). Although the simulated vortex is generally stronger, the change of the intensity excellently shows the process of rapid intensification from a tropical storm to a typhoon within 12 hours. The reason why the simulated vortex does not weaken as seen in later time points of the best track (after 42 hours) is because the simulated storm moves slower than observed. The simulated storm and the best track share the same feature of near-equatorial genesis, short lifetime, rapid intensification, and rapid weakening.

From the simulated radar reflectivity and the satellite observations in the horizontal plane (Fig. 5), a small and compact near-equatorial typhoon is well illustrated. The simulated typhoon has a small and clear eye with a diameter of 50 km, which is in agreement with the observations. The detailed structure

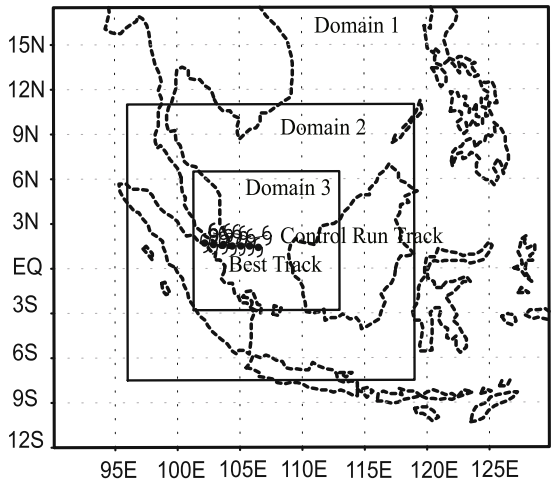

Fig. 3. Simulation domains, simulated typhoon track, and JTWC best track of Typhoon Vamei at 6-hourly intervals from 1200 UTC 26 Dec to 0000 UTC 28 December 2001.

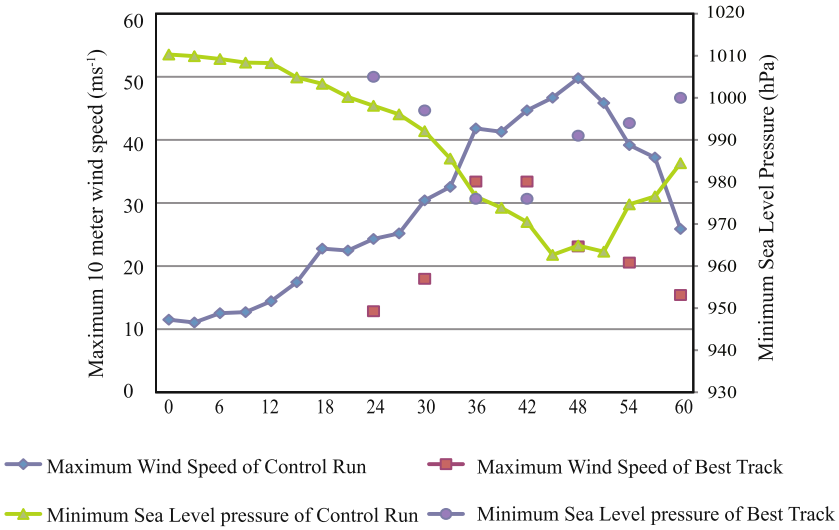

Fig. 4. Comparison of the intensity of the simulated typhoon (9 km resolution domain) and the JTWC best track (maximum 10-meter wind speed and minimum sea level pressure).

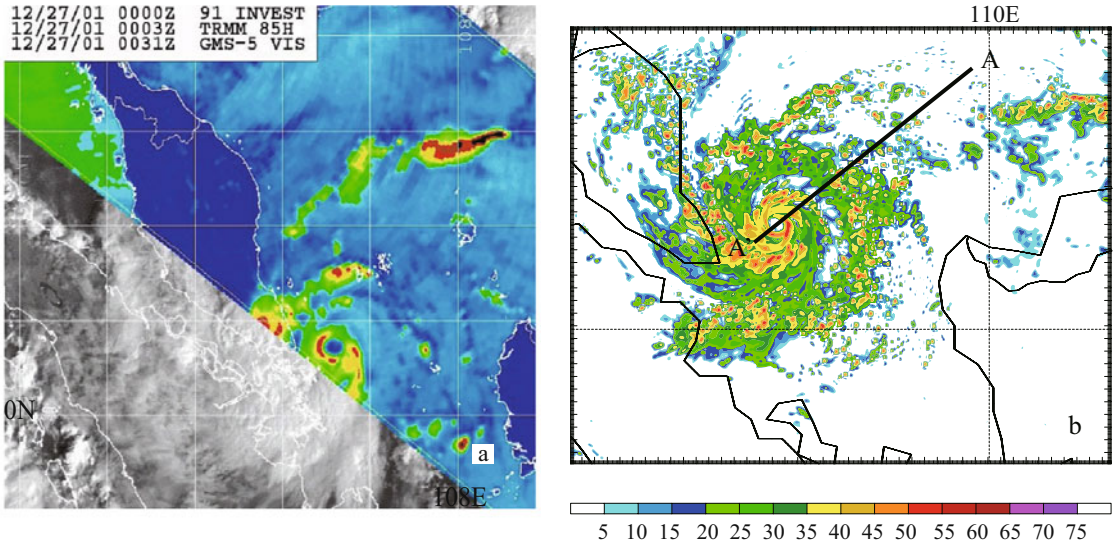

Fig. 5. (a) Observed structure of Typhoon Vamei from TRMM and GMS5 observations at 0300 UTC 27 December 2001 (adapted from JTWC 2001 annual tropical cyclone report); (b) radar reflectivity at 36 hours (valid at 0000 UTC 27 December 2001) of the simulation in the 3-km domain. AA' is a line in the 9-km resolution domain.

of the surrounding typhoon spiral rainbands in the 3 km domain is clearly shown to consist of many organized mesoscale convective vortexes.

5. Discussions

As noted before, prior researchers have noted that wind surges play an important part in providing cyclonic vorticity (Chang et al., 2003). But specifically, how does a wind surge act to increase the cyclonic vorticity to the whole column? What are the key properties of such a strong wind surge? Is there any other effect from the wind surge apart from the dynamical contribution? In order to answer these questions, it is very much necessary to investigate the vertical structure of the atmosphere. We set a fixed vertical section along the line AA' (see Fig. 5b), which extends from the north-east point A to the equatorial point A' in the southwest direction. About 6 hours before Vamei intensified into a typhoon, line AA' passes just through the typhoon circulation center.

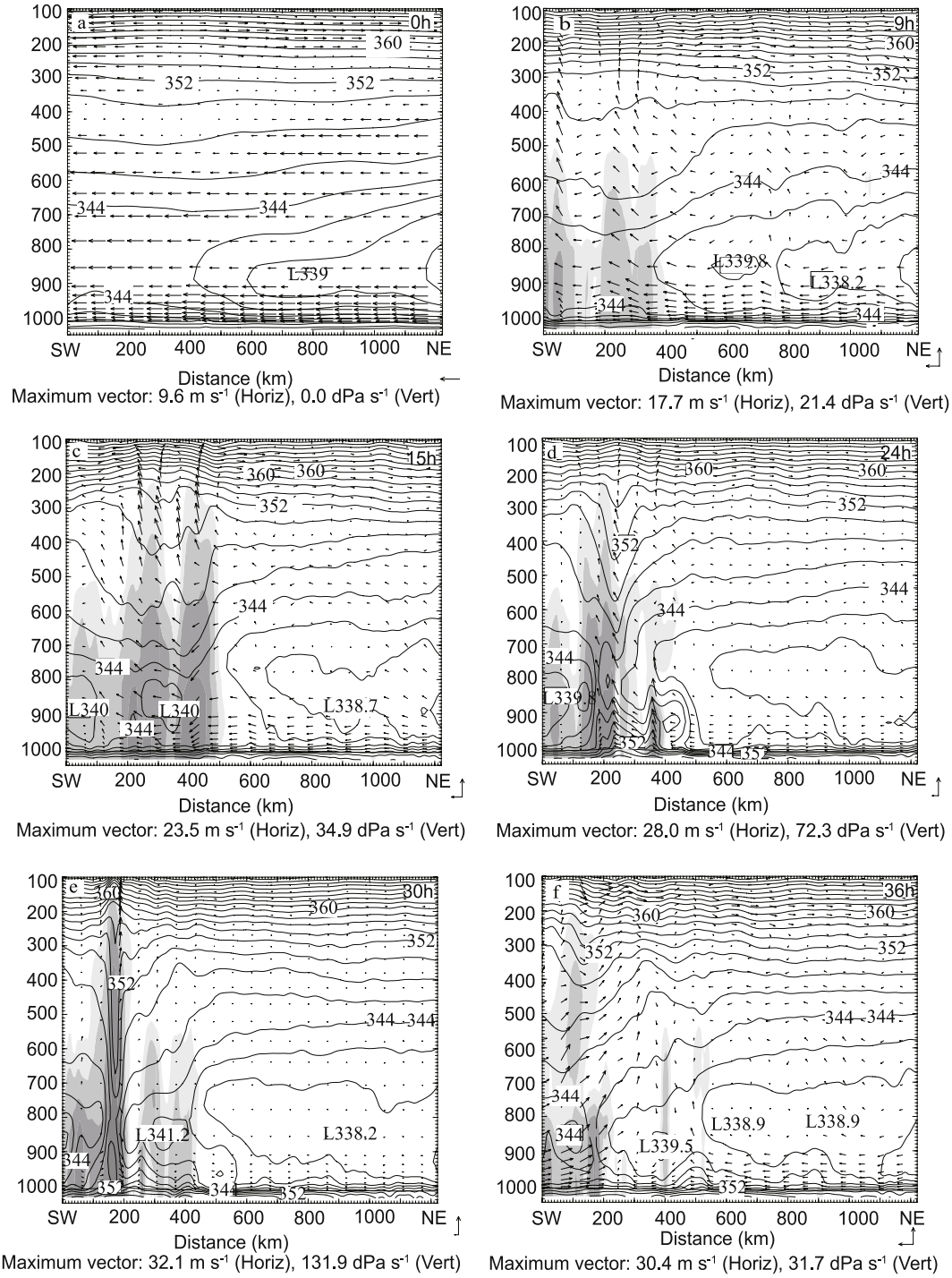

Fig. 6. Simulated EPT (contours, units: K), wind circulation vector, and radar reflectivity (shaded, units: dBZ) on vertical sections along line AA' for: (a) 0 hours, (b) 9 hours, (c) 15 hours, (d) 24 hours, (e) 30 hours, and (f) 36 hours in domain 3. The vectors at the right-bottom corner of each panel denote the scale of velocity in horizontal and vertical direction.

5.1 *Thermal effect—Hints from the equivalent potential temperature structure on vertical sections*

Firstly, we try to determine the equivalent potential temperature (EPT) on the vertical sections along line AA'. It is widely acknowledged that EPT is a parameter which can indicate both warm/cold and dry/humid properties of air masses. From the very start of the simulation, it is evident from Fig. 6a that there is a layer representing a strong dry/cold wind intrusion from the northeast centered at 850 hPa. After 9 hours of model integration, the wind surge (denoted by the 340 K contour) drifts slightly to lower latitudes and splits into two parts: the majority of the wind surge occurs from the north and a small portion of the air mass goes to the south. At 15 hours, the smaller portion of wind surge (denoted by the low EPT centered at 340 K) enters the southern warm and humid area. At the same time, the simulated radar reflectivity denotes an abrupt eruption of convection. Upward vertical motion also experiences a period of rapid increase. Through hours 24, 30, and 36, the separated wind surges continue to take effect as the typhoon intensifies. It is thus anticipated that the presence of a low-mid-level cold and dry wind surge helps to increase instability underneath, contributing to the development of convective outbreaks.

5.2 *Dynamic effect—Hints from diagnosis of terms in vorticity equation*

From the above description, the strong wind surge plays an important part in the formation of near-equatorial Typhoon Vamei (2001). But what makes the vorticity of the typhoon increase? In what way does the wind surge contribute to the increase of vorticity? Based on the results of the simulation, we try to answer the question by analyzing the vorticity budget. The average vorticity is calculated over a 10×10 grid point box (domain 2, about 90 km×90 km) centered on the minimum sea level pressure point.

After Holton (2004), the vorticity equation in an isobaric system can be written as:

$$\frac{\partial \xi}{\partial t} = -\left(u\frac{\partial \xi}{\partial x} + v\frac{\partial \xi}{\partial y}\right) - \beta v - \omega\frac{\partial \xi}{\partial p} - (f+\xi)\nabla\cdot\boldsymbol{V} - \left(\frac{\partial \omega}{\partial x}\frac{\partial v}{\partial p} - \frac{\partial \omega}{\partial y}\frac{\partial u}{\partial p}\right) \quad (1)$$

Here, u, v, ω are the zonal, meridional, and vertical velocities respectively; ζ denotes relative vorticity. On the right side of the equation, the terms from left to right are terms for horizontal vorticity advection, planetary vorticity advection, vertical vorticity, divergence, and tilting. Because the planetary vorticity advection term is about 2 orders of magnitude smaller than the other terms, we neglect it in the analysis.

Similar to the discussions in Chambers and Li (2007), the divergence term and horizontal advection term can be combined together to get a horizontal vorticity flux term:

$$\zeta_{\text{flux}} = -\frac{\partial}{\partial x}(u\zeta) - \frac{\partial}{\partial y}(v\zeta) \quad (2)$$

This term directly shows the true variation of horizontal vorticity in the area.

Figures 7a–e shows the contribution of different terms in the vorticity equation at 900 hPa, 850 hPa, 800 hPa, 500 hPa, and 200 hPa, respectively, and Fig. 7f shows the average vorticity around the typhoon center. At the early stages of typhoon genesis, the vorticity at 900 hPa increases first at 18 hours, which is 3 hours after cold surge enter the southern warm and humid area (Fig. 6c) and stays the highest among all levels; as Vamei (2001) intensifies into a typhoon, the vorticity at 800 hPa and 850 hPa surpasses that at 900 hPa. At most of the levels, the changes of vorticity correspond well to the changes of typhoon intensity (as illustrated by the "Max Wind" line in Fig. 7f).

At 900 and 850 hPa (Figs. 7a, b), the terms in the vorticity equation show similar characteristics, except that the vorticity contribution at 900 hPa is larger than at 850 hPa. The convergence term has the most important positive contribution at these two levels, while the largest negative contribution comes from the advection term, and the sum of the two terms (the horizontal vorticity flux) also shows an upward increase. Thus, the convergence term is the most important source in the increase of vorticity at the lower levels. However, between 850 and 800 hPa, the sign of the contribution from the convergence term is reversed. The horizontal relative vorticity advection term takes the place of convergence term and becomes the largest positive vorticity contribution. Instead, the convergence term turns into the largest negative contribution term. Furthermore, the vertical vorticity term and the tilting term are relatively important compared to the situation at the lower levels. Evidently, the horizontal advection term plays the dominant role in the middle levels of the troposphere. When it comes to 200 hPa, all terms in the vorticity equation tend to be of the same order of magnitude.

In summary, the vorticity changes within the lower levels of the troposphere are associated with corresponding changes in typhoon intensity. The positive vorticity advection from the wind surge only makes contribution to the vorticity budget of Vamei (2001) above 800 hPa, below which the major vorticity source comes from the convergence term in the boundary

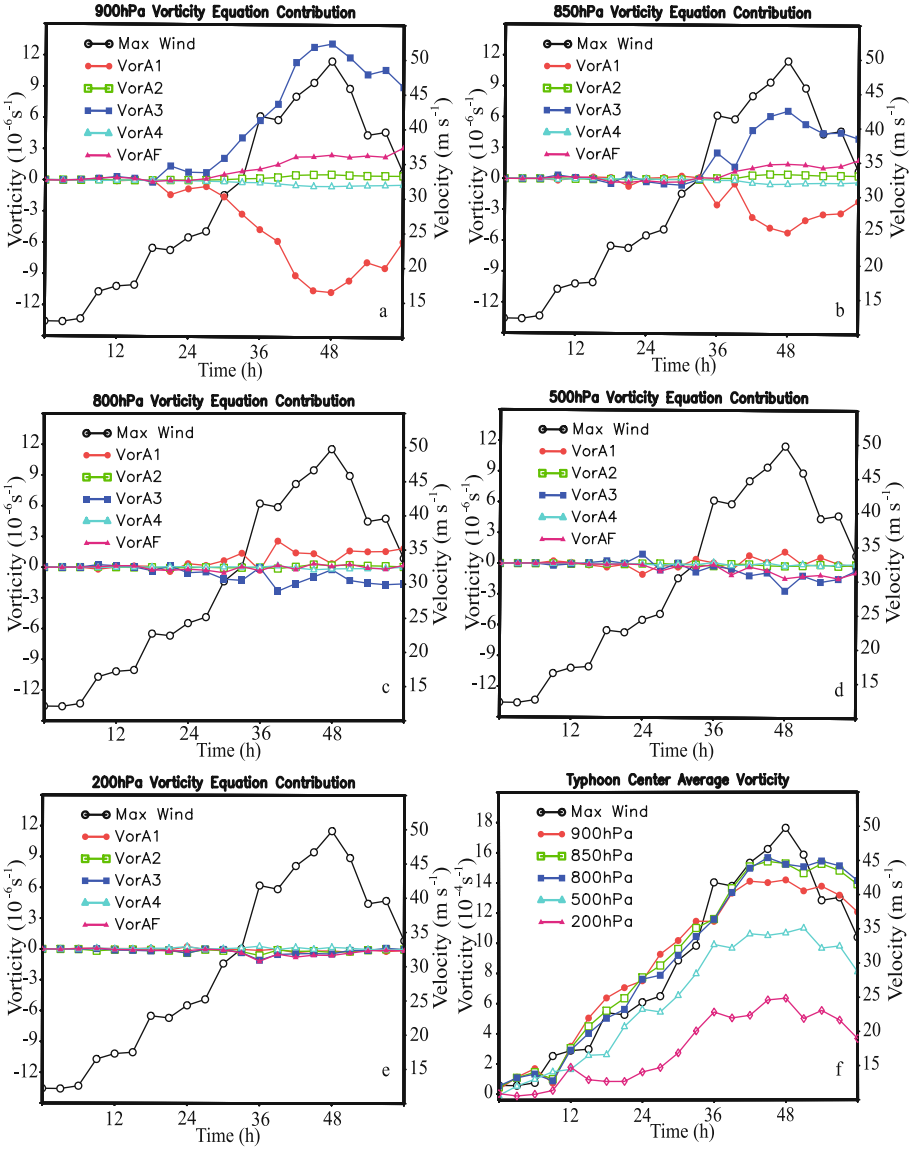

Fig. 7. The contribution of different terms in the vorticity equation at (a) 900 hPa, (b) 850 hPa, (c) 800 hPa, (d) 500 hPa, (e) 200 hPa and the average vorticity around typhoon center (f), where Max wind denotes the maximum wind of the simulated typhoon. VorA1 is the horizontal vorticity advection term; VorA2 is the vertical vorticity term; VorA3 is the divergence term; VorA4 is the tilting term; VorAF is the horizontal vorticity flux term (VorA1+VorA3).

layer. The advection of the cold wind surge over the warm ocean boundary provides a more favorable condition for the outbreaks of convection, which may help to induce strong convergence near the boundary layer.

5.3 *Sensitivity experiments about the genesis of Vamei*

Besides the aforementioned effect, there are still other potential factors in Vamei's (2001) genesis. For instance, several studies (Chang et al., 2003 and Chambers and Li, 2007) have suggested that the unique terrain distribution of the south-east Asian region may be potentially important. By way of numerical sensitivity experiment, we try to determine the role of such factors.

5.3.1 *Analysis of sensitivity experiments on terrain and land-sea distribution*

Many former studies have pointed out that the terrain around southeast Asia, especially near Luzon, can coherently have effects on the wind surge in the winter of the northern hemisphere, thus contributing to a

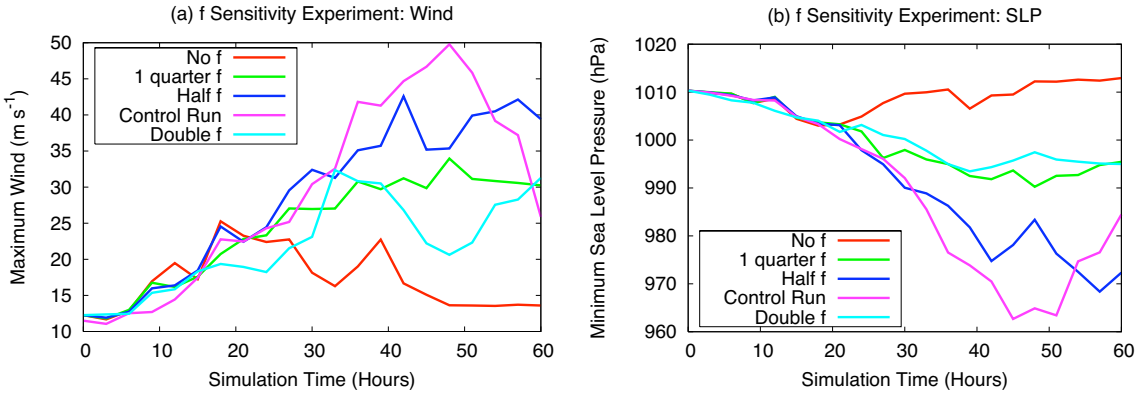

Fig. 8. (a) Simulated maximum wind and (b) sea level pressure of sensitivity experiments on Coriolis parameter (f).

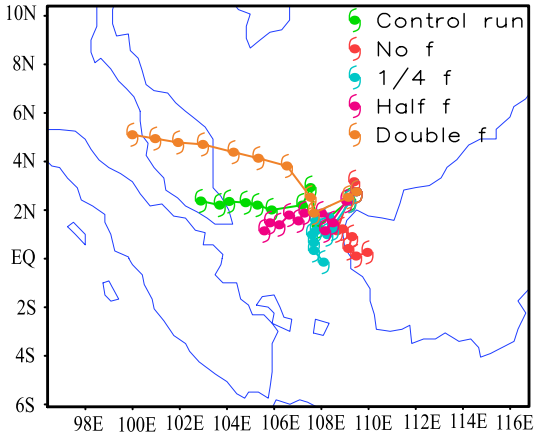

Fig. 9. The simulated tracks of the sensitivity experiments on Coriolis parameter (f).

series of convection events and disturbances on the leeward side. Chang et al. (2003) believed that the narrows of the South China Sea and the mountainous terrain of Borneo present a rare situation whereby near-equatorial typhoons can not occur elsewhere. Chambers and Li (2007) also state that the blocking effect of the terrain near the Vamei (2001) genesis region forces the wind surge from the north to rotate anti-clockwise and helps to build up the cyclonic vortex in the typhoon genesis region. In theory, the V-shaped terrain distribution in Southeast Asia can have a kind of "tunneling effect" which causes the wind passing through to intensify. In order to ascertain the extent to which the terrain may affect near-equatorial typhoon genesis, a set of numerical sensitivity experiment is designed.

The set of experiment has two tests and one control run. In Terrain test 1, all the terrain in the initial field in the model is removed and is set to zero height. The initial field in Terrain test 2 changes all land surfaces to sea surfaces on the basis of Terrain test 1.

The results of simulations (figures not shown) show that tropical cyclones in these experiments all have maximum winds of more than 32.9 m s^{-1} (typhoon strength). The trends of intensity variation show very small differences except in Terrain test 2 the typhoon does not weaken because there is no landfall. Interestingly, there seems to be nearly no effect when the terrain is removed; whereas replacing land with sea has a relatively larger influence on the simulated typhoon intensity. As for the simulated typhoon tracks, they all relatively drift to the north and the simulated typhoon in Terrain test 2 moves much more rapidly.

As a conclusion, it is speculated that the terrain and land-sea distribution have very limited effects on the genesis of Typhoon Vamei in this case study. Their effect is more evident on the track and intensity after the typhoon has formed. In other words, even if the terrain and land-sea distribution, are rather different, near-equatorial typhoons can still form. Our results based on statistical study of near-equatorial typhoons throughout recent history supports this conclusion to some extent. It shows that areas of open sea far from land are the locations where the majority of near-equatorial typhoons are formed.

5.3.2 *Analysis of sensitivity experiments on the Coriolis parameter (f)*

Anthes (1982) has stated that tropical cyclones can only gain effective rotation outside of 6 degrees off the equator. And Emanuel (2003) believed that tropical cyclones should form under conditions of non-zero absolute vorticity. The main reason for their statements is that the Coriolis parameter is clearly advantageous to the genesis of vorticity in tropical cyclones. In this section, we try to assess the effects of the Coriolis parameter (f) by numerical sensitivity experiments. Is f completely irrelevant if relative vorticity is sufficiently large? Or can it not be ignored? This set of experiments includes five tests with: f=0, one-quarter f, half f, doubled f, and the control run, respectively.

Figure 8 gives the intensity of the simulated typhoons and Fig. 9 shows the tracks of the typhoons in the different tests.

The result shows that if the Coriolis parameter (f) is reduced to zero, the tropical cyclone can no longer intensify into a typhoon (Fig. 11). But if f is reduced to one-quarter of its original value, or is increased by a factor of two, typhoon intensity can still be reached, but is much weaker. The most similar test result compared to the control run is the half-f test.

The simulated tracks also show a very interesting result (Fig. 9). As the Coriolis parameter is larger, the simulated track drifts to the north; when the Coriolis parameter is smaller, the track drifts equatorward. The one-quarter f test demonstrates that a typhoon can even move across the equator and enter the other hemisphere.

Although in reality the Coriolis parameter (f) for a particular storm could never be modified, this experiment at least gives us some hints about this force's role in typhoon genesis. The Coriolis parameter should be neither too large nor too small in order for Vamei (2001), at least, to intensify into a typhoon. The Coriolis parameter and the wind surge both make contributions to the track of Vamei. If f is much larger, Vamei tends to move poleward. If f is too small, then the wind surge tends to play the dominant role and drives the typhoon system towards the equator.

6. Conclusions

Near-equatorial tropical cyclones represent a very small class of all tropical cyclones, but their genesis mechanism is important, since these cases may define the extreme conditions for tropical cyclone genesis dynamics. The climatology of near-equatorial typhoons over the western-north Pacific is fully investigated using the JTWC typhoon record from 1951 to 2006. Almost all the near-equatorial typhoons occurred in winter and spring, and an 11-year cycle of higher frequency of near-equatorial typhoons is found in the WNP. Relative humidity at mid-levels and wind surges at lower levels are found to be anomalous prior to near-equatorial typhoon genesis over the WNP.

By implementing a fine resolution model simulation, the role of wind surges on the genesis of near-equatorial Typhoon Vamei (2001) is analyzed. The model results demonstrate that WRF can simulate a near-equatorial typhoon without an initial bogus vortex. The track of the simulated typhoon is located relatively further north compared with observations (about 0.5°). The simulated intensity of Vamei is in agreement with the observations.

It is found from a fixed vertical section from the northeast to the southwest that the wind surge invades the middle-low levels, but does not extend to the surface. Then, small groups of air currents with low equivalent potential temperature are separated from the majority of the air mass. These groups of cold/dry air are transported by the wind surge over the warm/humid air mass in the low latitude area. These intrusions help to increase the instability and initialize the convective outburst. The diagnosis of the vorticity equation shows that the variation of vorticity at the lower levels corresponds to the change of typhoon intensity. The main source of vorticity lies in the lowest layers of the atmosphere. The dominant term with a positive contribution is the divergence term at the lower boundary layer and the advection term near the middle levels.

The sensitivity experiments related to terrain and land-sea distribution demonstrate that these factors play very limited role in the genesis of Vamei (2001). More importantly, they affect the track and speed of typhoon. The experiments related to the Coriolis parameter (f) show that although f may be small, it is still important in the genesis and evolution of Vamei (2001) due to the domination of this factor's contribution to the track of Vamei (2001).

This case study shows the possible roles of wind surge, terrain, the land-sea distribution, and the Coriolis force on tropical cyclone genesis, but attribution of the detailed dynamical processes behind Vamei (2001) are still not completely settled. More observational and numerical studies are greatly needed to fully understand the dynamical processes responsible for near-equatorial typhoon genesis.

Acknowledgements. This study is supported by Chinese State Key program 2009CB421500, the National Natural Science Foundation of China under Grant Nos. 40921160380 and 40975059, and the Scientific Research Foundation of the Ministry of Education of China. The authors would like to thank two anonymous reviewers for their helpful comments and suggestions in the improvement of the manuscript.

REFERENCES

Anthes, R. A., 1982: *Tropical Cyclones: Their Evolution, Structure and Effects. Meteorological Monographs*, 208pp.

Chambers, C. R. S., and T. Li, 2007: Simulation of formation of a near-equatorial typhoon Vamei (2001). *Meteorol. Atmos. Phys.*, **98**, doi: 10.1007/s00703-006-0229-0.

Chang, C. P., C. H. Liu, and H. C. Kuo, 2003: Typhoon Vamei: An equatorial tropical cyclone formation. *Geophys. Res. Let.,* **30**(50), 1–4.

Chen, F., and J. Dudhia, 2001: Coupling an advanced land-surface/ hydrology model with the Penn State/ NCAR MM5 modeling system. Part I: Model description and implementation. *Mon. Wea. Rev.*, **129**, 569–585.

Emanuel, K., 2003: Tropical cyclones. *Annual Review of Earth and Planet Sciences*, **31**, 75–104.

Fortner, L. E., 1958: Typhoon Sarah, 1956. *Bull. Amer. Meteor. Soc.*, **39**, 633–639.

Gray, W. M., 1968: Global view of the origin of tropical disturbances and storms. *Mon. Wea. Rev.*, **96**, 669–700.

Gray, W. M., 1998: The formation of tropical cyclones. *Meteorol. Atmos. Phys.,* **67**, 37–69.

Holliday, C. R., and A. H. Thompson, 1986: An unusual near-equatorial typhoon. *Mon. Wea. Rev.*, **114**, 2674–2677.

Holton, J. R., 2004: *An Introduction to Dynamic Meteorology.* Academic Press, 4th ed., 535pp.

Janjic, Z. I., 2002: Nonsingular implementation of the Mellor–Yamada Level 2.5 Scheme in the NCEP Meso model. NCEP Office Note, No. 437, 61pp.

Joint Typhoon Warning Center, cited 2009: Annual Tropical Cyclone Report, Joint Typhoon Warning Center, Pearl Harbor, HI, 2002. [Available online at http://www.npmoc.navy.mil/jtwc/atcr/atcr_archive.html]

Juneng, L., F. T. Tangang, C. J. Reason, S. Moten, and W. A. Hassan, 2007: Simulation of tropical cyclone Vamei (2001) using the PSU/NCAR MM5 model. *Meteor. Atmos. Phys.*, **97**, doi: 10.1007/s00703-007-0259-2.

Kain, J. S., and J. M. Fritsch, Eds., 1993: Convective parameterization for mesoscale models: The Kain-Fritcsh scheme. *The Representation of Cumulus Convection in Numerical Models*, Amer. Meteor. Soc., 246pp.

Kalnay, E., and Coauthors, 1996: The NCEP/NCAR 40-year reanalysis project. *Bull. Amer. Meteor. Soc.*, **77**, 437–470.

Kanamitsu, M., W. Ebisuzaki, J. Woollen, S.-K. Yang, J. J. Hnilo, M. Miorino, and G. L. Potter, 2002: NCEP-DOE AMIP-II Reanalysis (R-2). *Bull. Amer. Meteor. Soc.*, **83**, 1631–1643.

Lin, Y.-L., R. D. Farley, and H. D. Orville, 1983: Bulk parameterization of the snow field in a cloud model. *Journal of Climate and Applied Meteorology*, **22**, 1065–1092

Skamarock, W. C., J. Klemp, J. Dudhia, G. David, B. Dale, W. Wang, and J. Powers, 2007: A description of the advanced research WRF Version 2. NCAR/TN-468+STR, NCAR Technical Note, Boulder, Colorado, USA.

Smith, T. M., R. W. Reynolds, T. C. Peterson, and J. Lawrimore, 2008: Improvements to NOAA's historical merged land–ocean surface temperature analysis (1880–2006). *J. Climate*, **21**, 2283–2296.

Stauffer, D. R., and N. L. Seaman, 1994: On multi-scale four-dimensional data assimilation. *J. Appl. Meteor.*, **33**, 416–434.

Wang, G., J. Su, Y. Ding, and D. Chen, 2007: Tropical cyclone genesis over the South China Sea, *Journal of Marine Systems*, **68**, 318–326.